Journal of Applied Sciences and Nanotechnology, Vol. 2, No. 2 (2022)

Journal of Applied Sciences and Nanotechnology

Journal homepage: https://jasn.uotechnology.edu.iq/

Nanoplasmonic Sensing Using Gold Nanostructures

[1]Abbas A. Thajeel, [1]Mohammed A. Ibrahem*, [2]Duha S. Ahmad

[1]Laser Sciences and Technology Branch, Department of Applied Sciences, University of Technology – Iraq

[2]Applied Physics Branch, Department of Applied Sciences, University of Technology – Iraq

Article information

Article history:
Received: September, 16, 2021
Accepted: February, 20, 2022
Available online: June, 10, 2022

Keywords:
Plasmonic effect,
Gold nanostructures film,
CeO_2 nanoparticles,
Plasmonic nanosensing

Corresponding Author:
Mohammed A. Ibrahem
mohammed.a.ibrahem@uotechnology.edu.iq

Abstract

Nanoplasmonic sensing, based on the plasmonic resonance absorption of thin, irregularly-shaped Au nanostructures film, with a starting thickness of about 15 nm (±3 nm) sputtered on a quartz substrate, is used to monitor the CeO_2 NPs (with an average diameter of 50 nm) film refractive index variations using different film thicknesses (90 nm, 146 nm, 172 nm, and 196 nm). Increasing the film thickness of solution-processed CeO_2 NPs film, with layer-by-layer deposition on top of Au nanostructures, shows a significant redshift in the plasmonic resonance absorption of the plasmonic metal, from 580 nm to 611 nm. Such an increase is related to the change in the building microstructure of the semiconductor's film which is reflected in changing its refractive index. Plasmonic surface refractive index sensitivity of 437.5 nm/RIU with FOM of 4.2 has been recorded. Such a sensing technique offers a large potential for developing cost-effective plasmonic nanosensing devices for clinical applications. This sensor structure is versatile and can be utilized to sense and monitor a large variety of materials and chemicals.

DOI: 10.53293/jasn.2021.4282.1087, Department of Applied Science, University of Technology

1. Introduction

Plasmonic sensors and read-out devices have witnessed a significant increase in their use in various research sectors, especially in biosensing and catalysis applications [1][2]. The field of plasmonics is first introduced by the German physicist Gustav Mie in 1908 [3]. However, the important works in the field of localized surface plasmonic resonance (LSPR) are only being introduced a decade ago [4]. The significance of the plasmonic effect is due to its unique optical behavior resulting from the confined optical interaction of metal's free charge carriers with the incident electromagnetic field. Such an interaction stimulates a strong plasmonic field in a very small area (beyond the diffraction limit) leading to strong absorption and scattering processes of the incident light at the resonance wavelength of the metal nanostructures [5][6][7]. The plasmonics effect is normally characterized by a couple of inherent factors like the metal's type, structure, and dimension. However, another important factor, which highly affects the plasmonic resonance absorption, is the refractive index of the media surrounding the metal nanostructures[8] [9]. The influence of this factor can normally be recognized by causing a shift in the plasmonic absorption peak with any slight variation in the refractive index of the surrounding medium [10]. Two different plasmonic sensing techniques were used to record this plasmonic resonance sensitivity namely; direct and indirect plasmonic sensing [11]. The earlier is based on a direct interaction of the

plasmonic metal with the material or medium of interest (analyte), where any change in this material (inside or at the surface) can be indicated by the change in the plasmonic resonance response of the metal. On the other hand, the indirect plasmonic sensing is based on isolating the metal nanostructures with a buffer layer where any change in its refractive index, as a result of the surface interaction with the analyte (the studied material), leads to a shift in the plasmonic resonance absorption [12][13][14].

Optical sensing based on the plasmonic effect is a rapidly developing field and can be divided into two main techniques; surface plasmon resonance (SPR) and localized surface plasmonic resonance (LSPR). The earlier method is based on propagating the electric field at the metal-dielectric interface while the latter is based on the confined plasmonic field resulting from an isolated metal nanostructure. The sensing device configuration and their sensing capabilities in both techniques are different. SPR technique is beyond the scope of this work and therefore will not be discussed further. A good overview of the physics of plasmonics can be found in this review [15]. LSPR is first being used in biosensing applications, specifically for DNA and proteins by Mirkin [16] and Englebienne [17] respectively. Silver nanostructures (Ag) show a significant plasmonic resonance cross-section and are therefore considered as an excellent choice in plasmonic nanosensing applications [18]. However, its plasmonic efficiency is found to be rapidly damped by the fast formation of the oxide layer which affects its long-term stability in ambient conditions. Therefore, as a reliable alternative, gold nanostructures (Au) are found to be the Nobel metal of choice because of their corrosion resistance and can be used with many other materials and solvents [19]. The plasmonic resonance of Au nanostructures can easily be tuned from the visible to the near-IR based on the preparation technique. One simple and cost-effective method to prepare Au nanostructures is by thermal deposition or sputtering of a very thin film on low adhesion substrates such as glass and quartz. It has been found that Au nanostructures prepared by such methods show high sensitivity to the surrounding medium [20]. This study provides crucial insight and proves of concept towards utilizing the plasmonic effect to determine surface interactions as well as monitoring the change in film thickness through a wavelength shift of the plasmonic resonance of anisotropically-shaped Au nanostructures. A simple yet efficient nanoplasmonic sensing chip is utilized based on a planar device configuration to maximize the sensitivity capabilities of our measurement. This work aims to provide a proof of concept of plasmonic sensitivity based on changing the optical properties of the surrounding medium and use it to monitor the change in CeO_2 refractive index as a result of changing its film thickness. It also provides a thorough analysis of the sensor performance utilizing a simple yet efficient sensor configuration.

2. Experimental Procedure

A gold nanostructured film having a thickness of 15 nm (±3 nm), is deposited on top of the 1×1-cm quartz substrate by the sputtering process. A quartz substrate is cleaned thoroughly, by the ultrasonic bath, using three consecutive solutions; acetone, ethanol, and distilled water, and then dried by a stream of hot air before Au film deposition. The clean substrates were then transferred to the sputtering chamber. Au foil (purity of 99.99%) was used as a sputtering target in a SPC-12 plasma sputtering coater system with a DC of 10 mA for the sputtering time of 20 sec and base pressure of 2×10^{-4} torr. The sputtering process is performed under inert Ar gas with a pressure of 3 mTorr. The deposited Au film is used as it is without any further heating treatment. A suspension of Cerium (IV) oxide (CeO_2) NPs, with an average particle diameter of 50 nm (± 5 nm) purchased from Sigma-Aldrich, in deionized water with a concentration of 3% by weight, was spin-cast on top of the Au nanofilm using a spin coater from HOLMARC (model: HO-TH-05) with spinning speed of 2500 rpm at maximum acceleration for 30 sec in air. 4 different CeO_2 NPs films were deposited, layer-by-layer, on top of the Au film following the same deposition procedure, each of which was thermally treated at 100 $^{\circ}$C for 10 min in the air using the hot plate to remove any residual water. The plasmonic resonance absorption of Au nanostructures, before and after the deposition of CeO_2 NPs films of different thicknesses, were measured, in the spectral range from 350 – 900 nm, using a UV-Vis (UV-1800, Shimadzu) spectrophotometer. The film thickness of different CuO_2 films was measured by the DektakXT profilometer from Bruker with ± 5 nm error expectation. Surface morphology of Au nanostructured film is examined using the Atomic Force Microscope (AFM, NT-MDT Spectrum Instruments) and the AFM image was analyzed using Gwyddion (version 2.47), a free available commercial AFM image analysis software. While the topography of CeO_2 NPs film was monitored using the Field Emission-Scanning Electron Microscope (FE-SEM, Mira 3- XMU).

3. Results and Discussion

3.1 Physical Characterization

The sensing mechanism utilized in this work is based on the direct nanoplasmonic sensing method where plasmonic nanostructures are in direct (physical) contact with the studied medium or film. Herein, the Au nanostructured film with a thickness of 15 nm (±3 nm) sputtered on a quartz substrate and then completely embedded in the layer-by-layer deposition of CeO_2 NPs films. The quartz substrate, Au nanostructured film as well as the CeO_2 NPs film are considered here as the nanoplasmonic sensing chip. The nanoplasmonic sensitivity is measured by recording the optical response (plasmonic absorption) of the Au nanostructured film with the film thickness of the deposited CeO_2 NPs films.

A schematic representation of the nanoplasmonic sensing chip investigated here is shown in Figure (1-A). The thickness of the Au nanostructured film was kept fixed while the thickness of the CeO_2 films is varied by a 4 layer-by-layer deposition process which increasing the film thickness from 90 nm, 146 nm, 172 nm to 196 nm. FE-SEM image (Figure 1-B) shows that the deposited CeO_2 NPs are spherical with a diameter around 50 nm. The film is porous which is normal when using a spin coater deposition technique of a powder suspension.

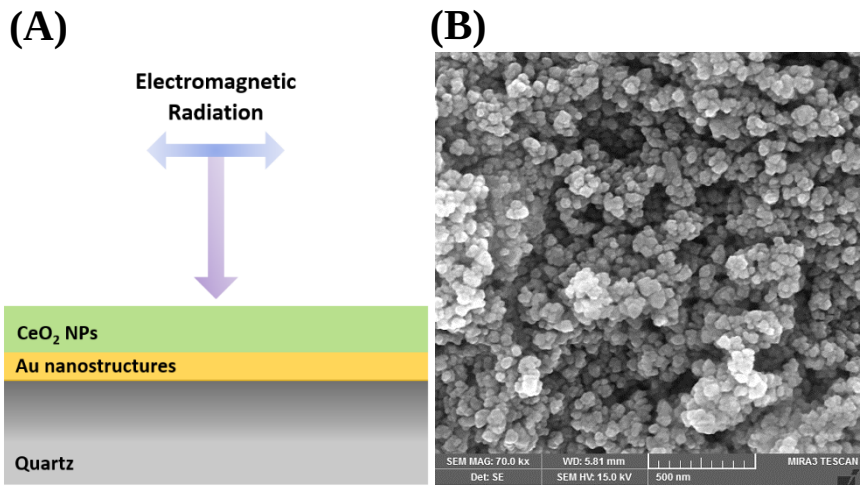

Figure 1: (A) A schematic illustration of the structural configuration of the nanoplasmonic sensing chip. (B) FE-SEM image of CeO_2 NPs film.

Figure 2-A shows an AFM image of the Au nanostructured film deposited on a quartz substrate without any further heating treatment. The inset in Figure 2-A shows an optical photo of the quartz substrate covered with Au nanofilm while Figure 2-B shows a size distribution histogram of Au nanostructures extracted using Gwyddion AFM image processing software. The average area of the deposited Au nanostructures (islands) was estimated to be around 33 nm (±2 nm) as indicated by fitting the size distribution data in Figure 2-B. These randomly distributed shapes and sizes of Au nanostructures gave the Au nanostructured film its unique dark greenish color which resulted from having different localized surface plasmonic resonance responses with different particle sizes and structures [21].

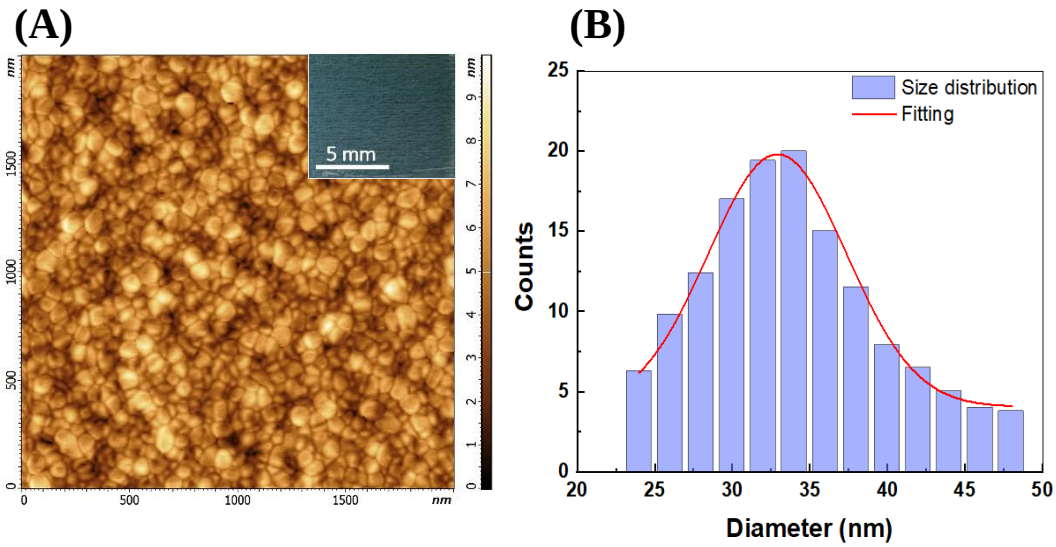

Figure 2: (A) AMF image of Au nanostructures film deposited on top of the quartz substrate. The inset shows an optical photograph of the Au nanostructured film. (B) size distribution histogram of Au nanostructures obtained from the AFM image.

3.2 Nanoplasmonic Sensing

Optical sensing by LSPR is a phenomenon that is affected by combined factors such as the electronic density of the used metal nanostructures, size, and shape as well as the refractive index of the environment near the metal nanostructures [22]. Any change in one of these factors can efficiently be detected by simply measuring the plasmonic resonance either by transmission or absorption spectra. Plasmonic sensitivity measurement is performed by varying the refractive index of the surrounding medium by changing the CeO_2 film thickness. Figure 3-A shows the optical absorption of CeO_2 films of different thicknesses deposited on quartz substrates (surface treated with 100 °C for 10 min before recording the optical absorption) without Au nanostructures. The optical refractive index of CeO_2 of different thicknesses have been calculated utilizing the following equation [23][24]:

$$n = \left[\frac{(1+R)}{(1-R)}\right] + \sqrt{\frac{4 \times R}{(1-R)^2} - K^2} \quad (1)$$

Where n is the optical refractive index, which measures the light velocity when passing the testing medium, R is the CeO_2 film reflectance (computed from the transmission (T) and absorption (A) spectra: $R = 1 - (A + T)$)[25][26], and K is the extinction coefficient which is a function of the film's absorption coefficient (α) and given by: $K = \alpha\lambda/4\pi t$ [25].

Figure 3-B shows the optical refractive index as a function of the wavelength of CeO_2 films of different thicknesses. Results clearly show a big variation in refractive index values with increasing the film thickness from 90 nm to 196 nm. This variation in refractive index can efficiently be detected by the plasmonic effect of Au nanostructures. Figure 3-C shows the plasmonic resonance absorption spectra of Au nanostructured film before and after depositing 4 layers of CeO_2 NPs films (all CeO_2 NPs layers are deposited following the same deposition procedure of CeO_2 films mentioned earlier). The spectra show the characteristic plasmonic resonance absorption peak of Au nanostructures with values red-shifted with increasing the CeO_2 film thickness. The plasmonic resonance absorption peak of the as-deposited Au nanostructured film (without CeO_2 film), is located at 580 nm. The deposition of 1 layer of CeO_2 NPs film with a thickness of 90 nm on top of Au nanostructured film causes the plasmonic resonance peak of Au nanostructures to shift 7 nm towards longer wavelengths at 587

nm. Further increasing the film thickness of CeO_2 to 146 nm, 172 nm, and 196 nm, with layer-by-layer deposition, forcing the plasmonic resonance absorption peaks to shift to 593, 600, and 611 nm respectively.

These spectral shifts in the plasmonic resonance absorption of Au nanostructures are a direct consequence of refractive index variation where changing the CeO_2 film thickness on top of Au nanostructured film changes the CeO_2 film homogeneity (structures). The value of the refractive index of thin films is found to be significantly affected by the deposition technique and processing conditions which influence the structural characteristics of the film [27][28]. Figure 3-D shows the plasmonic sensitivity response with changing the surrounding medium the refractive index. The propagating surface plasmons show a non-linear increment with refractive index variation which is expected for a conventional flat gold film [29]. Results clearly show the direct dependence of plasmonic resonance peak position on the refractive index of the surrounding medium.

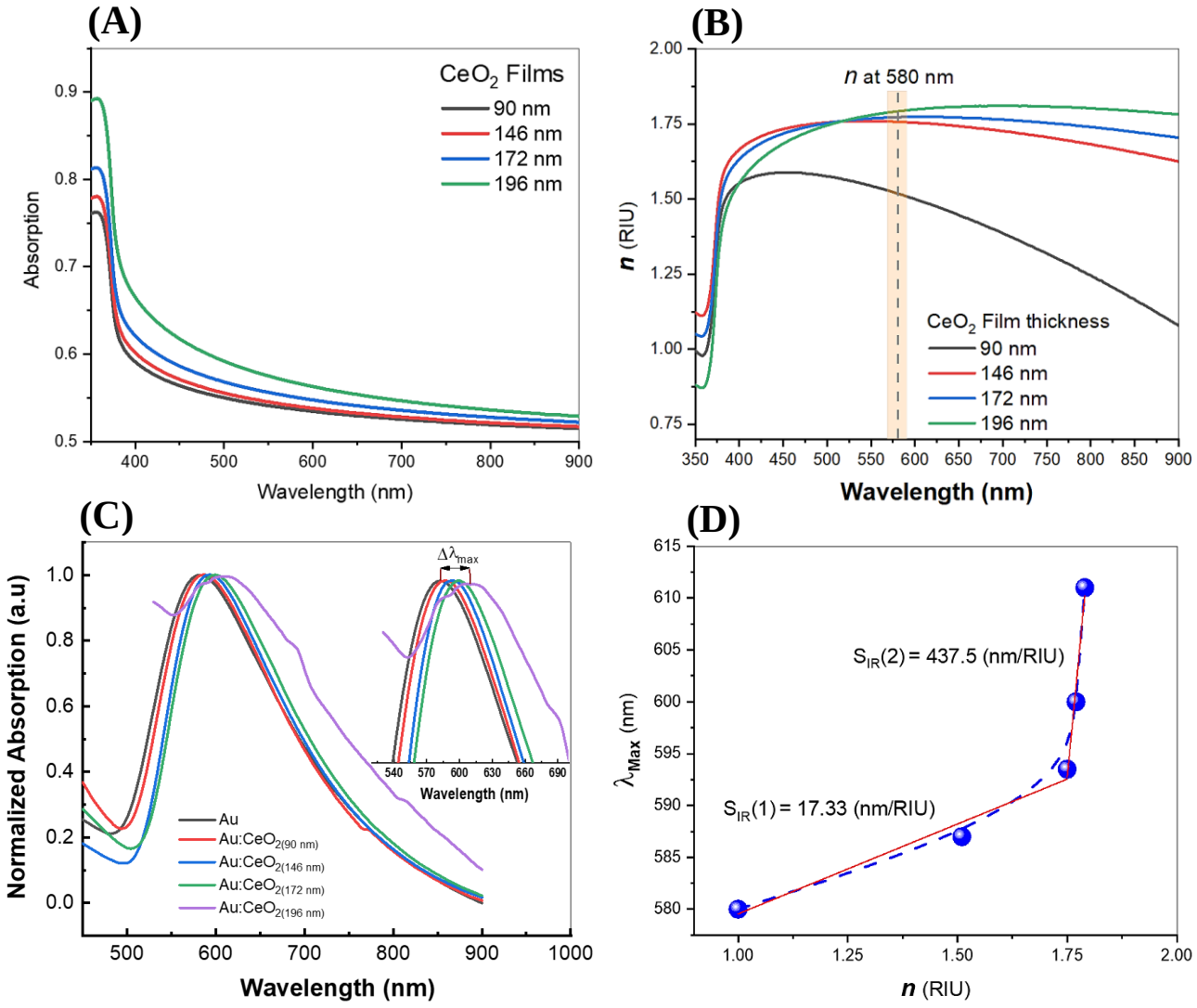

Figure 3: (A) Showing the absorption spectra of CeO_2 films deposited, layer-by-layer, on top of quartz substrate with different thicknesses. (B) Refractive index of CeO_2 films of different thicknesses derived from the absorption spectra. (C) Plasmonic resonance absorption of Au nanostructured film with multilayers of CeO_2 NPs films. (D) The plasmonic resonance peak position of Au nanostructures corresponds to the different refractive indexes of CeO_2 films. The peak position is extracted from (C) while refractive index values at 580 nm (resonance absorption of Au film) are extracted from (B).

To quantativly study the behaviour of our plasmonic sensor, surface refractive index sensitivity (S_{RI}) with a unit of (nm/Refractive Index Unite (RIU)), defined as the shifts in the plasmonic resonance peak position ($\Delta\lambda_{Max}$) as a function to the variation in refractive index (Δn) of the surrounding medium, is determined using the following equation [30][8]:

$$S_{RI} = \frac{\Delta\lambda_{Max}}{\Delta n} \tag{2}$$

Surface refractive index sensitivity (S_{RI}) is thus determined from the slop of Figure 3-D. The sensitivity shows two sensitivity regions, low and high with different sensitivity values; 17.33 nm/RIU and 437.5 nm/RIU respectively. Our plasmonic refractive index sensor is also characterized, taking into account the variation in size and shapes of the deposited Au nanostructures, by determining the figure of Merit (FOM) which accurately describe the performance of our sensor in respect to the resonance peak line-width, using the following equation [9][31]:

$$FOM = \frac{S_{RI}}{FWHM} \tag{3}$$

High values of the FOM mean that a smaller variation in the refractive index can be detected. Figure 4 shows the FOM of our plasmonic sensing device relative to variation in the surrounding refractive index of thin Au nanostructured film. Our sensor configuration shows a FOM of 4.2 when refractive index variation of 0.02 (n changed from 1.77 to 1.79) which is very high compared to others [32]. This is due to the variation of Au sizes and shapes which results in the high plasmonic wave penetration depth and hence high detection capabilities. Generally, the localized plasmonic resonance of Au nanostructures does not only depend on the physical shapes and sizes but also depend on the charge polarization capability of the interfaced medium [31]. When this medium or film has a high refractive index (high dielectric function), the electric charge of the exciting metal nanostructures, due to the excitation by the resonance wavelength, will be attenuated leading to reduce the restoring force of charges in the exciting metal. Such a reduction in the restoring force reduces the plasmonic resonance frequency leading to a redshift of plasmonic resonance towards longer wavelengths with the refractive index. Increasing the film thickness of CeO_2 NPs film leads to having a non-uniform microstructure which alters the film optical constants leading to change in its refractive index.

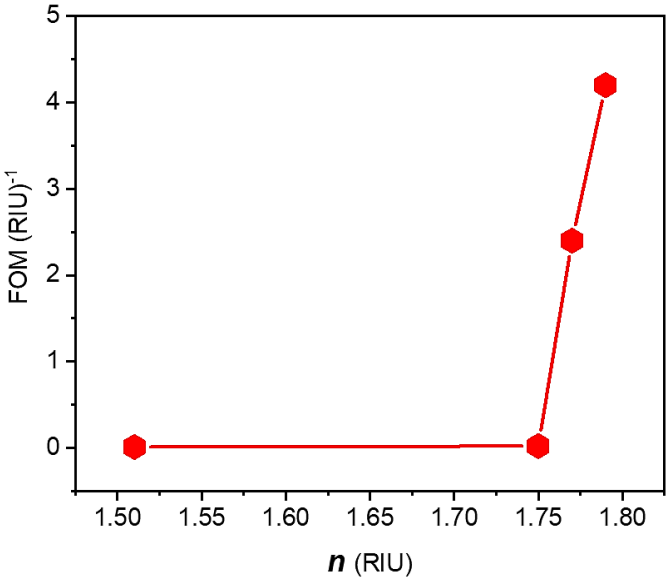

Figure 4: Shows the surface sensitivity and FOM of our plasmonic sensor relative to the variation in the refractive index of CeO_2 films.

4. Conclusions

We efficiently demonstrated a practical technique utilizing a simple yet effective configuration structure to investigate the effect of film thickness on the refractive index of CeO_2 NPs film and consequently on the plasmonic resonance absorption of Au nanostructured film. We showed that the plasmonic resonance of Au nanostructures is highly sensitive to any small changes in the refractive index of the surrounding medium. Increasing the thickness of CeO_2 NPs film changes its refractive index which shifts the plasmonic absorption peak position of Au nanostructures towards longer wavelengths. Optical responses of collective plasmonic resonant Au nanostructures at different environments enable this technique to be used in different applications including but not limited to biosensing.

Conflict of Interest:

The authors declare that they have no conflict of interest.

References

[1] P. S. S. dos Santos, J. M. M. M. de Almeida, I. Pastoriza-Santos, and L. C. C. Coelho, "Advances in Plasmonic Sensing at the NIR—A Review," *Sensors*, vol. 21, no. 6, p. 2111, Mar. 2021.

[2] F. Shaik, I. Peer, P. K. Jain, and L. Amirav, "Plasmon-Enhanced Multicarrier Photocatalysis," *Nano Lett.*, vol. 18, no. 7, pp. 4370–4376, 2018.

[3] G. Mie, "Beiträge zur Optik trüber Medien, speziell kolloidaler Metallösungen," *Ann. Phys.*, vol. 330, no. 3, pp. 377–445, 1908.

[4] T. Kume, N. Nakagawa, S. Hayashi, and K. Yamamoto, "Interaction between localized and propagating surface plasmons: Ag fine particles on Al surface," *Solid State Commun.*, vol. 93, no. 2, pp. 171–175, Jan. 1995.

[5] L. Wang, M. Hasanzadeh Kafshgari, and M. Meunier, "Optical Properties and Applications of Plasmonic-Metal Nanoparticles," *Adv. Funct. Mater.*, vol. 30, no. 51, p. 2005400, Dec. 2020.

[6] M. J. Kale, M. J. Kale, T. Avanesian, and P. Christopher, "Direct Photocatalysis by Plasmonic Nanostructures Direct," no. May, 2016.

[7] Y. Wang, E. W. Plummer, and K. Kempa, "Foundations of Plasmonics," *Adv. Phys.*, vol. 60, no. 5, pp. 799–898, Oct. 2011.

[8] Y. Zhao, S. Gan, G. Zhang, and X. Dai, "High sensitivity refractive index sensor based on surface plasmon resonance with topological insulator," *Results Phys.*, vol. 14, p. 102477, Sep. 2019.

[9] J. K. Bhattarai, M. H. U. Maruf, and K. J. Stine, "Plasmonic-Active Nanostructured Thin Films," *Processes*, vol. 8, no. 1, p. 115, Jan. 2020.

[10] H. Wang, "Plasmonic refractive index sensing using strongly coupled metal nanoantennas: nonlocal limitations," *Sci. Rep.*, vol. 8, no. 1, p. 9589, Dec. 2018.

[11] C. Langhammer, E. M. Larsson, B. Kasemo, and I. Zorić, "Indirect Nanoplasmonic Sensing: Ultrasensitive Experimental Platform for Nanomaterials Science and Optical Nanocalorimetry," *Nano Lett.*, vol. 10, no. 9, pp. 3529–3538, Sep. 2010.

[12] F. Liu, X. Zhang, K. Li, T. Guo, A. Ianoul, and J. Albert, "Discrimination of Bulk and Surface Refractive Index Change in Plasmonic Sensors with Narrow Bandwidth Resonance Combs," *ACS Sensors*, vol. 6, no. 8, pp. 3013–3023, Aug. 2021.

[13] K. H. Aboud, N. Jamal Imran, and S. M. H. Al-Jawad, "Structural, Optical and Morphological Properties Cadmium Sulfide Thin Films Prepared by Hydrothermal Method," *J. Appl. Sci. Nanotechnol.*, vol. 1, no. 2, pp. 49–57, Jul. 2021.

[14] K. Chahrour, P. Choon Ooi, and A. A. Hamzah, "Influence of the Voltage on Pore Diameter and Growth Rate of Thin Anodic Aluminium Oxide (AAO) Pattern on Silicon Substrate," *J. Appl. Sci. Nanotechnol.*, vol. 1, no. 2, pp. 10–15, Jul. 2021.

[15] M. L. Brongersma, N. J. Halas, and P. Nordlander, "Plasmon-induced hot carrier science and technology," *Nat. Nanotechnol.*, vol. 10, no. 1, pp. 25–34, 2015.

[16] C. A. Mirkin, R. L. Letsinger, R. C. Mucic, and J. J. Storhoff, "A DNA-based method for rationally assembling nanoparticles into macroscopic materials," *Nature*, vol. 382, no. 6592, pp. 607–609, Aug. 1996.

[17] P. Englebienne, "Use of colloidal gold surface plasmon resonance peak shift to infer affinity constants from the interactions between protein antigens and antibodies specific for single or multiple epitopes," *Analyst*, vol. 123, no. 7, pp. 1599–1603, 1998.

[18] Q. Wang and L. Wang, "Lab-on-fiber: plasmonic nano-arrays for sensing," *Nanoscale*, vol. 12, no. 14, pp. 7485–7499, 2020.
[19] N. Sarfraz and I. Khan, "Plasmonic Gold Nanoparticles (AuNPs): Properties, Synthesis and their Advanced Energy, Environmental and Biomedical Applications," *Chem. – An Asian J.*, vol. 16, no. 7, pp. 720–742, Apr. 2021.
[20] S. Badilescu, D. Raju, S. Bathini, and M. Packirisamy, "Gold Nano-Island Platforms for Localized Surface Plasmon Resonance Sensing: A Short Review," *Molecules*, vol. 25, no. 20, p. 4661, Oct. 2020.
[21] S. J. Henley, M. J. Beliatis, V. Stolojan, and S. R. P. Silva, "Laser implantation of plasmonic nanostructures into glass," *Nanoscale*, vol. 5, no. 3. pp. 1054–1059, 2013.
[22] I. Kaminska *et al.*, "Near-Field and Far-Field Sensitivities of LSPR Sensors," *J. Phys. Chem. C*, vol. 119, no. 17, pp. 9470–9476, Apr. 2015.
[23] S. B. Aziz *et al.*, "Synthesis of PVA/CeO2 Based Nanocomposites with Tuned Refractive Index and Reduced Absorption Edge: Structural and Optical Studies," *Materials (Basel).*, vol. 14, no. 6, p. 1570, Mar. 2021.
[24] F. Yakuphanoglu, G. Barım, and I. Erol, "The effect of FeCl3 on the optical constants and optical band gap of MBZMA-co-MMA polymer thin films," *Phys. B Condens. Matter*, vol. 391, no. 1, pp. 136–140, Mar. 2007.
[25] S. B. Aziz *et al.*, "Structural and Optical Characteristics of PVA:C-Dot Composites: Tuning the Absorption of Ultra Violet (UV) Region," *Nanomaterials*, vol. 9, no. 2, p. 216, Feb. 2019.
[26] E. T. Salim, Y. Al-Douri, M. S. Al Wazny, and M. A. Fakhri, "Optical properties of Cauliflower-like Bi 2 O 3 nanostructures by reactive pulsed laser deposition (PLD) technique," *Sol. Energy*, vol. 107, pp. 523–529, Sep. 2014.
[27] F.-C. Chiu and C.-M. Lai, "Optical and electrical characterizations of cerium oxide thin films," *J. Phys. D. Appl. Phys.*, vol. 43, no. 7, p. 075104, Feb. 2010.
[28] Y. Han, X. Huang, A. C. W. Rohrbach, and C. B. Roth, "Comparing refractive index and density changes with decreasing film thickness in thin supported films across different polymers," *J. Chem. Phys.*, vol. 153, no. 4, p. 044902, Jul. 2020.
[29] E. Martinsson *et al.*, "Local Refractive Index Sensing Based on Edge Gold-Coated Silver Nanoprisms," *J. Phys. Chem. C*, vol. 117, no. 44, pp. 23148–23154, Nov. 2013.
[30] S. Szunerits and R. Boukherroub, "Sensing using localised surface plasmon resonance sensors," *Chem. Commun.*, vol. 48, no. 72, p. 8999, 2012.
[31] Y. Xu *et al.*, "Optical Refractive Index Sensors with Plasmonic and Photonic Structures: Promising and Inconvenient Truth," *Adv. Opt. Mater.*, vol. 7, no. 9, p. 1801433, May 2019.
[32] J.-F. Masson, "Portable and field-deployed surface plasmon resonance and plasmonic sensors," *Analyst*, vol. 145, no. 11, pp. 3776–3800, 2020.